Science of the Total Environment 631–632 (2018) 534–549

Contents lists available at ScienceDirect

Science of the Total Environment

journal homepage: www.elsevier.com/locate/scitotenv

Heat waves in Portugal: Current regime, changes in future climate and impacts on extreme wildfires

J. Parente [a,*], M.G. Pereira [a,c], M. Amraoui [a], E.M. Fischer [b]

[a] Centre for Research and Technology of Agro-Environment and Biological Sciences, CITAB, University of Trás-os-Montes and Alto Douro, Portugal
[b] Institute for Atmospheric and Climate Science, ETH Zurich, Switzerland
[c] Instituto Dom Luiz, Faculdade de Ciências da Universidade de Lisboa, Lisboa, Portugal

HIGHLIGHTS

- Central Portugal present the highest heat wave (HW) amplitude in 1981–2010 period.
- NE and S of Portugal have the highest heat wave number and duration.
- Extreme fire occurrence is clearly associated with HWs' characteristics.
- 97% of total number of extreme fires were active during HWs.
- Higher increase in all HWs' characteristics by the end of the 21st century

GRAPHICAL ABSTRACT

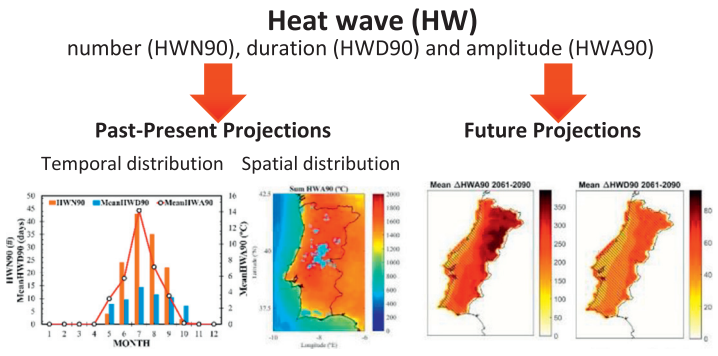

ARTICLE INFO

Article history:
Received 22 December 2017
Received in revised form 27 February 2018
Accepted 5 March 2018
Available online xxxx

Editor: Wei Huang

Keywords:
Heat wave
Extreme wildfire
Climate variability
Climate change
Portugal

ABSTRACT

Heat waves (HW) can have devastating social, economic and environmental impacts. Together with long-term drought, they are the main factors contributing to wildfires. Surprisingly, the quantitative and objective analysis leading to the identification and characterization of HW in current and future climate conditions as well as its influence on the occurrence of extreme wildfires (EW) has never been performed for Portugal and are the main objectives of this study. For this reason, we assess HW in recent past and future climate based on a consistent high resolution meteorological database and have compared their occurrence with long and reliable, precise and detailed information about Portuguese fire events. Results include the characterization of HW frequency, duration, seasonality and intensity for current and different future climate conditions and their relationship with EW occurrence. We detected 130 HW between 1981 and 2010, concentrated between May and October and highest values in July and August. The highest HW number and duration is found over the Northeast corner and the south of the country while highest amplitudes are typically located in central area. HW characteristics present high inter-annual variability but are clearly associated to the temporal and spatial distribution of EW: 97% of total number of EW were active during an HW, 90% of total EW days were also HW days; 82% of the EW had duration completely contained in the duration of an HW; and, 83% of EW occurred during and in the area affected by HW. Our results also show that HW should increase in number, duration and amplitude, more significantly for RCP 8.5, and for the 30-year periods near the end of the 21st century. Findings of this study will support the definition of climate change adaptation strategies for fire danger and risk management.

* Corresponding author at: Universidade de Trás-os-Montes e Alto Douro, Quinta de Prados, 5000-801 Vila Real, Portugal.
E-mail addresses: joanaparente@utad.pt (J. Parente), gpereira@utad.pt (M.G. Pereira), malik@utad.pt (M. Amraoui), erich.fischer@env.ethz.ch (E.M. Fischer).

https://doi.org/10.1016/j.scitotenv.2018.03.044
0048-9697/

1. Introduction

The World Meteorological Organization (WMO) and World Health Organization (WHO) define heat wave (HW) as an event of abnormally and uncomfortably hot weather over a large area, that usually lasts from a few days to a few weeks, with local thermal conditions recorded above given thresholds (McGregor et al., 2015; WMO, 2016). The subjectivity of this statement, in particular the absence of quantitative criteria to identify these events, their duration, amplitude and spatial extent, leads to more than one operational definition depending, for example, on the type of adverse effects of these spells (Cowan et al., 2014; Fischer and Schär, 2010; Gouveia et al., 2016; Gronlund et al., 2014; Jacob et al., 2014; Perkins et al., 2012; Russo et al., 2015; Vautard et al., 2013).

Regardless of the definition used, the social, economic and environmental impacts of HW can be catastrophic. For example, consequences of summer 2003 HW in Europe included the death of thousands of vulnerable people, a huge number of heat-stroke cases, excess emergency visits and hospital admissions which overwhelmed hospitals' capabilities (De Bono et al., 2004; Dhainaut et al., 2004; Fouillet et al., 2006; Gronlund et al., 2014; McGregor et al., 2015).

Environmental and economic impacts of HW 2003 include, but are not restricted, to: (i) reduced pollen production, airborne pollen loads and pollen season (Gehrig, 2006); (ii) reduced alpine glacier's mass (Haeberli et al., 2004) and stability of rock walls leading to exceptional rock falls (Gruber et al., 2004); (iii) decreased agricultural production and heavy losses in crops which affected the food retailing sector (Chung et al., 2014; García-Herrera et al., 2010; van der Velde et al., 2010); (iv) increased demand for water and energy, that resulted in power shortages and even blackouts (Miller et al., 2008).

More than 25,000 fires were recorded in Europe during 2003 HW, mostly in southern (Portugal, Spain, Italy, France) but also in central and northern countries (e.g., Austria, Finland, Denmark and Ireland) which burned a total of 650,000 ha of forest, scrublands but also agricultural areas, mostly in Portugal, c.a. 390,000 ha (60% of total), the highest value ever recorded in the last decades (Costa et al., 2011; De Bono et al., 2004; Trigo et al., 2006). The estimated global financial impact of wildfires in Portugal exceeded 1 billion € while the joint impacts of drought and forest fires over Europe exceed 13 billion € (COGECA, 2003; De Bono et al., 2004). The increased fire incidence during 2003 HW had devastating effects on both the natural (air pollution and water quality degradation) and built environment (De Bono et al., 2004; Perkins et al., 2012). Impacts of other HWs on fires in Europe and other regions were also noticeable. In 2002, Russia was affected by an HW which favoured the occurrence of late season major fire outbreaks which results on total BA of 12,000,000 ha (Page et al., 2008). Gouveia et al. (2016) studied the synergy between drought, HWs and fuels as well as its impacts on the 2007 southern Greece exceptional fire season.

HW development is mainly due to the presence of a persistent high pressure system, driving anticyclonic advection of hot air and leading to high isolation and air temperature (Bador et al., 2017; Duchez et al., 2016; Krueger et al., 2015) as well as the inhibition of precipitation events (Vautard et al., 2013), which increase the likelihood of EWs' occurrence (Perkins et al., 2012) especially in the Mediterranean basin (Hernandez et al., 2015). In fact, weather and climate are important drivers on all stages of fires (Barbero et al., 2015; Parente et al., 2016; Pereira et al., 2005; Tedim et al., 2018). At large spatial-temporal scale, climate helps to determine the presence, type and life cycle of vegetation while hot and dry weather increase fuels' dryness and flammability (Blarquez et al., 2015; Flannigan et al., 2016; Parente et al., 2016; Pereira, 2015). The Mediterranean type of climate, stimulates the vegetation existence and development, during the wet and mild winters and springs, and promotes the vegetation thermal and hydric stress, during the hot and dry summers (Pereira et al., 2013). Summer weather conditions in mainland Portugal are strongly influenced by the position and magnitude of the Azores anticyclone, which controls the general atmospheric circulation and the advection of dry and warm air from either Continental Europe or the Sahara desert (Dasari et al., 2014; Tedim et al., 2018). These conditions help to understand the fire incidence intra-annual variability, namely the higher number of fires and BA during summer months (Telesca and Pereira, 2010; Trigo et al., 2006). For these reasons, Portugal mainland is particularly vulnerable to the occurrence of extremely high temperatures that may lead to the occurrence of HWs and EWs (Andrade et al., 2014).

Observed and projected climate change as well as the diversity and magnitude of HWs impacts motivated researchers to assess the eventual existence of trends in HWs characteristics temporal evolution (Cowan et al., 2014), to evaluate the ability of regional climate models to accurately simulate HWs at regional scale (Vautard et al., 2013), to estimate HW occurrence for different climate change scenarios (Russo et al., 2015) and future changing patterns of European HW frequency, amplitude and duration (Fischer and Schär, 2010) as well as for impact assessment and adaptation in Europe (Jacob et al., 2014). However, to the best of our knowledge, there is no study performed for Portugal about the characteristics of HWs in the recent past, projections for the future climate and about the influence of HWs on the occurrence of EWs. Therefore, this study has three main objectives: (i) to characterize and analyse the evolution of HWs over Portugal in present climate conditions (1981–2010); and, (ii) for future climate scenarios and periods; as well as (iii) to assess the role of HW on EW occurrence.

2. Materials

2.1. Study area

Continental Portugal shares the Iberian Peninsula with Spain with whom it has border to the north and east, and faces the Atlantic Ocean in its West and South coast. Tagus River broadly divides Continental Portugal into northern and southern regions with approximately equal area but very different environmental characteristics (Fig. 1). Portugal has a temperate type of climate, where the summer is dry, i.e. precipitation value <40 mm, and hot in the south and warm in the north (Kottek et al., 2006). Weather conditions in mainland are strongly influenced by: (i) the position and magnitude of the Azores anticyclone, (ii) the moderating effect of the Atlantic Ocean and, (iii) the influence of the Mediterranean Sea and North Africa (Dasari et al., 2014; Tedim et al., 2018). The northern region has a more irregular topography and higher altitudes (2,000 m near *Penhas Douradas*), denser river network and higher fraction of forest vegetation cover while southern region is characterized by lower altitudes, high aridity and the predominance of agricultural areas (Parente and Pereira, 2016).

2.2. Data

2.2.1. Meteorological datasets

ERA-Interim is a gridded global atmospheric reanalysis of climate observations. ERA-Interim dataset was selected to provide meteorological fields for 30-year climatological period defined between 1981 and 2010, here considered the control period. This third generation reanalysis dataset is the latest produced by the European Centre for Medium-Range Weather Forecasts using an improved atmospheric model and data assimilation to solve some inaccuracies of previous products (Dee et al., 2011). A large set of meteorological variables and related parameters are available at daily and sub-daily time steps since 1979 and continuously updated in almost real time and at a spatial resolution from 3° × 3° to 0.125° × 0.125° latitude/longitude, in spite the native resolution of ≈80 km which means that the downloaded dataset is an interpolation of the primary data source (Dee et al., 2011).

For this study, maximum air temperature at 2 m was extracted for a spatial domain (10°W–6°E, 36.5°N–42.5°N) centred in Continental Portugal with the highest spatial resolution. Then, daily maximum temperature (T_{max}) was computed from 8 × daily time series in each point of

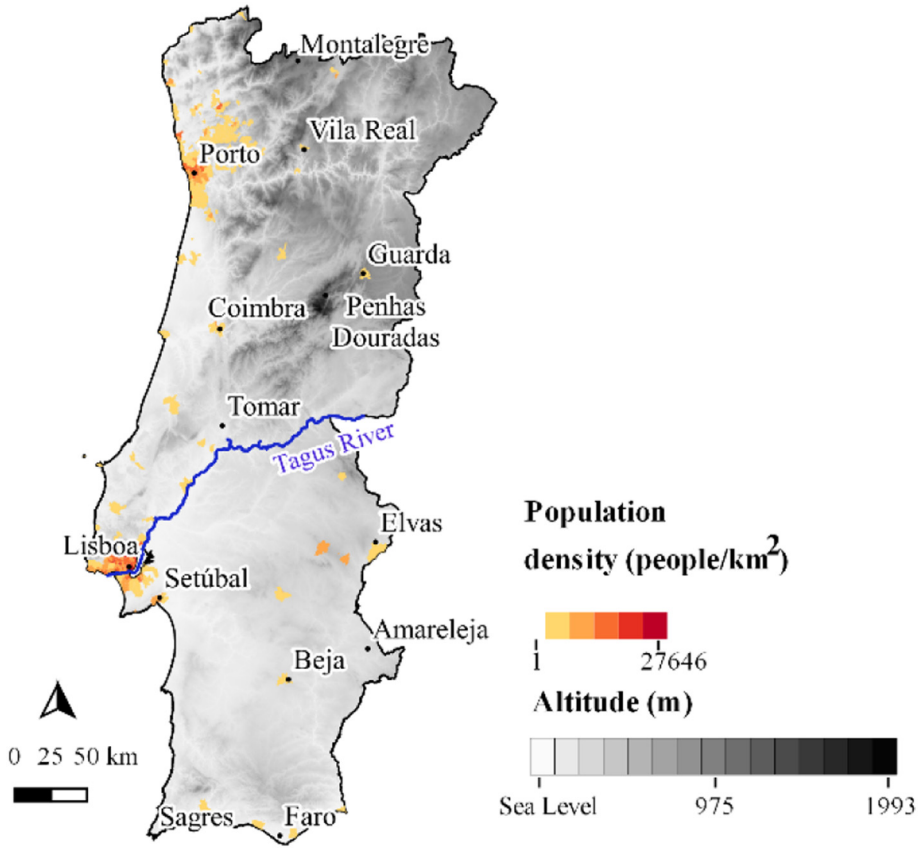

Fig. 1. Portugal geographical characterization including altitude, population density and the location of some selected cities and Tagus River.

ERA-Interim grid. Preliminary and exploratory statistical climatological analysis was performed to characterize T_{max} distribution which includes resistant and robust measures of location (median, Q2), dispersion (interquartile range, IQR) and extremes, namely the 10th (P10), 90th (P90), 95th (P95) and 99th (P99) percentiles. Q2 spatial pattern is essentially characterized by a North-South gradient, with higher values in the southern inland region, which reflects the combined influence of the latitude, continentally as well as the proximity to Africa and to Mediterranean Sea (Fig. 2, top left panel). On the other hand, IQR present an interior-coastal contrast clearly associated with the moderating effect of the Atlantic Ocean (Fig. 2, top central panel). The spatial distribution of extreme lower values of T_{max} (P10) reveal the existence of a SW-NE gradient, resembling the average mean air temperature pattern in winter (Fig. 2, top right). However, the extreme high values of T_{max} (P90, P95 and P99) present higher values in the interior south-centre region (Fig. 2, bottom panels).

Climate models have inherent deficiencies due to structural and parameterization uncertainties, missing processes, imperfect or simplified representation of lateral boundary conditions. Therefore, bias-adjusted past and future projections of regional climate models from the CORDEX (Coordinated Regional Climate Downscaling Experiment) Adjust project dataset (http://cordex.org/data-access/bias-adjusted-rcm-data/) were used to assess potential differences in HW occurrence and characteristics for future climate scenarios. The CORDEX-Adjust project contains a subset of EURO-CORDEX (European - CORDEX) simulations available for the new representative concentration pathways (RCP) 4.5 and 8.5 (WCRP CORDEX, 2016). The EURO-CORDEX initiative is one of the 15 parts of global CORDEX, that provides regional climate projections for Europe at 50 km (EUR-44) and about 12 km (EUR-11) resolution (Jacob et al., 2014; Ouzeau et al., 2016). The regional simulations are a physical downscaling of the CMIP5 (Coupled Model Intercomparison Project Phase 5) global climate projections. The global climate models were forced with RCP and are generally defined as follows (Van Vuuren et al., 2011): RCP 4.5 corresponds to a stabilization without overshoot of radiative forcing after 21st century at 4.5 $W.m^{-2}$ (~650 ppm CO_2 eq); and, RCP 8.5 consist on rising of radiative forcing pathway leading to 8.5 $W.m^{-2}$ (~1,370 ppm CO_2 eq) at the end of 21st century.

In this study, we used bias-adjusted simulations provided by the Swedish Meteorological and Hydrological Institute (SMHI) corrected with Distribution-Based Scaling (DBS45) bias-adjustment method (Yang et al., 2010) and using the regional reanalysis MESAN (EU FP7 EURO4M project) dataset (Landelius et al., 2016), for the EUR-11 CORDEX domain. In summary, we used T_{max} for: (i) the control period (1981–2010) and 5 different/consecutive 30-year future climatological periods (namely, 2021–2050, 2031–2060, 2041–2070, 2051–2080 and 2061–2090); (ii) two representative concentration pathways (RCP4.5 and RCP8.5); (iii) and, simulated by 3 pairs of General Circulation Model (GCM)/Regional Climate Model (RCM), namely, MOHC-HadGEM2-ES/RACMO22E, MOHC-HadGEM2-ES/CCLM4-8-17 and MPI-M-MPI-ESM-LR/REMO2009.

2.2.2. Fire datasets

The Portuguese forest national authority (*Instituto da Conservação da Natureza e das Florestas*, ICNF), provide two official and different fire datasets: (a) Portuguese Rural Fire Database, which is based on ground measurements, comprising, for each fire record, the fire location, BA and detailed information on ignition and extinction date and time of fire events (Pereira et al., 2011); and, (b) National Mapping Burnt Area, which is based on satellite imagery information and composed by BA polygons in an annual time scale (Parente et al., 2016). Information on both datasets were combined to enable the simultaneous availability of detailed spatial and temporal information about BA of the wildfires selected for this study. For reasons of simplicity and obvious need to limit the presentation to a reasonable amount of results obtained, this study will focus on EW here defined as fires with BA ≥5000 ha (Fig. 3).

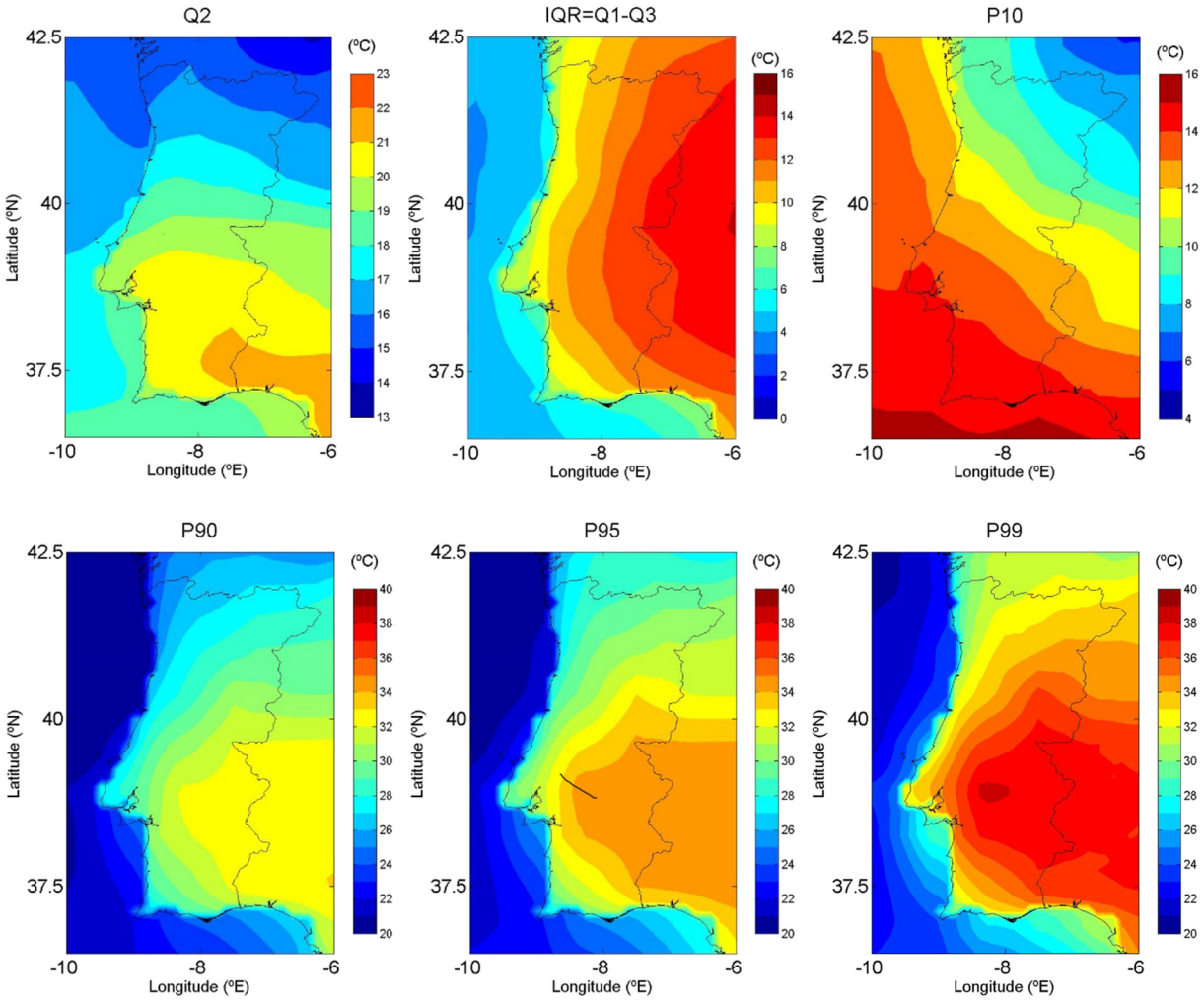

Fig. 2. Resistant and robust measures of the statistical distribution of the maximum air temperature including: the 10th percentile (P10), the median or second quartile (Q2), inter quartile range (IQR) as well as the 90th (P90), 95th (P95) and 99th (P99) percentiles in each grid point of the ERA-Interim reanalysis dataset (0.125° longitude × 0.125° latitude) spatial domain, for 30-year climatological period 1981–2010.

In fact, EW can be a much more complex phenomenon (Tedim et al., 2018) but for operational reasons we considered EW as extreme large wildfires. In the control period (1981–2010) a total of 62 EW occurred in Portugal, which corresponds to 0.02% of total number of wildfires but to almost 19% of total BA. This highlights the role of this small number of EW in the total BA in Portugal.

2.3. Methods

The Portuguese Institute of the Sea and Atmosphere (IPMA) considers an HW as a period of at least 6 consecutive days, where maximum daily temperature is 5 °C higher than the average daily value in the reference period (DGS, 2013). However, the Portuguese Heat–Health Warning System consider other criteria (e.g., ICARO warning index; maximum and minimum temperature; sudden rise in surface air temperature ≥ 6 °C; fire occurrence; exceedances of ozone levels; UV radiation levels; local events; weather warnings; Universal Thermal Climate Index) to define three alert levels. Since this study intends to evaluate and characterize the occurrence of HWs in Portugal as well as its relation with EWs, which are essentially a summer problem, we adopt the HW definition of Fischer and Schär (2010). Specifically, an HW consists in at least six consecutive days with $T_{max} > P90$, but without removing the seasonal cycle. This definition is especially suitable when it is desired to detect absolute extreme events of T_{max}, which naturally tend to occur during summer, and not relative events, such as those that may occur in each month or season of the year.

HWs criterion of existence and a set of descriptors to characterize the occurrence and magnitude of these air temperature extreme events were assessed in each grid point of the spatial domain. The list of descriptors includes the number (HWN90), duration (HWD90), frequency (HWF90) and amplitude (HWA90) of the HW. In each point, the duration of an HW is simply the total number of consecutive days with $T_{max} > P90$, if greater or equal 6. The frequency is simply the HW day frequency. The amplitude or intensity of an HW is the sum of the difference ($T_{max} - P90$) for all days of HW.

HWA90, HWD90 and HWF90 were computed for each HW and for each year and each month of the 30-year climatological control and future climate periods, by assigning the statistics to the month in which the HW started. To evaluate the amplitude of an HW, HWA90 in all the points of the region where the HW occurs, were added and attributed to the same HW. In this way, the HWA90 for each HW takes into account not only the difference $T_{max} - P90$ but also the extent of the area affected by the HW. The spatial distribution and temporal evolution of these indices were compared with the spatial-temporal distribution of EWs, which will help to understand the impact of HW on wildfire events.

Finally, the process of detection and characterization of HW was repeated for all models projections and their characteristics for future scenarios compared to those obtained for the reference period. To analyse

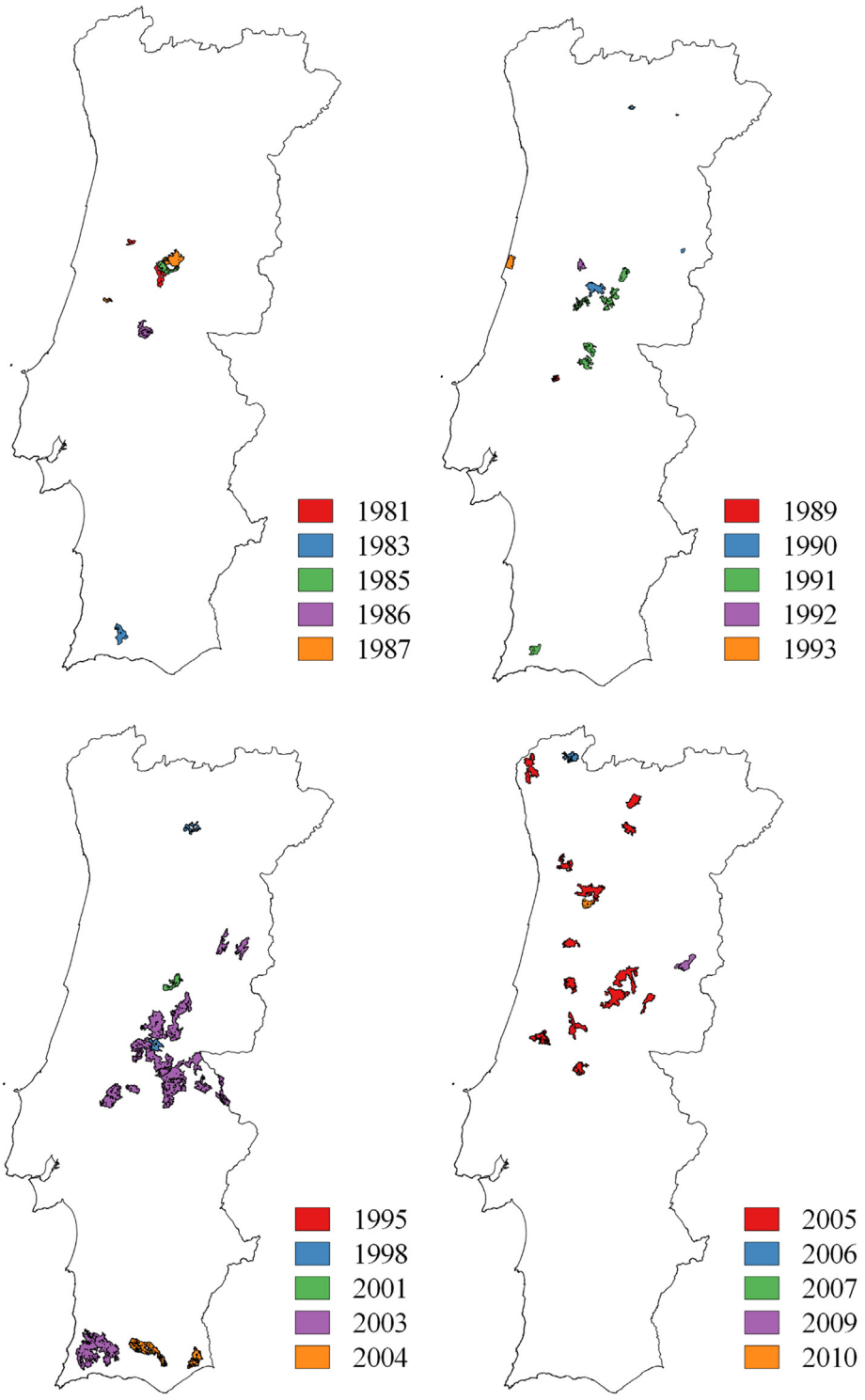

Fig. 3. Spatial and temporal distribution of extreme wildfires (burnt area ≥ 5,000 ha) between 1981 and 2010.

the robustness of the climate projections two statistical tests were performed (Jacob et al., 2014; Pfeifer et al., 2015). The first test – concordance – concerns the agreement of simulations in terms of the direction of change. The second – significance - regards the statistical significance of projected changes in each simulation, assessed by the Mann–Whitney–Wilcoxon test (Mann and Whitney, 1947; Wilcoxon, 1945). In this study, projected changes are considered robust when and where are simultaneously concordant (of the same sign) and statistically significant.

3. Results

3.1. HW characterization in the control period

Spatial patterns of total HWN90 and HWD90 for 1981–2010 period are relatively similar (Fig. 4, left and central panels). Higher values are located in the NE corner of the country and in the south region especially near the border with Spain. Apparently, the two larger metropolitan areas surrounding the two major cities (Lisbon and Porto) are the

regions less affected in terms of the number of HW. The region of Lisbon is also the less affected in terms of the number of HW days. Note that the model does not resolve the urban heat island effect, which may amplify the HWA90. The spatial distribution of total HWA90 is quite different from the other indices, much more homogeneous and, as expected, with higher values in continental inland regions, especially in the mountainous area near *Penhas Douradas* and at south of the city of *Tomar* (Fig. 4, right panel).

The intra- and inter-annual variability of HWs characteristics are also descriptors of HW regime. Monthly mean HWN90, HWD90 and HWA90 for the control period (Fig. 5) present a unimodal distribution that only exists between May and October, with higher frequency, duration and amplitude in July and, secondly, in August. The distribution of mean HWD90 is quite symmetric (skewness of 0.37), while mean HWN90 and mean HWA90 present a right skewed distribution (respectively, skewness equal to 1.2 and 1.9), which means that the highest values were observed before August. Mean HWA90 has a leptokurtic distribution (kurtosis >0), which means higher probability of having extreme values than the other two descriptors with platykurtic distributions.

Annual distribution (Fig. 6) reveal high inter-annual variability, with highest values in 1981 and 2009 for HWN90, in 1990 and 2006 for HWD90, and in 1990 and 1992 for HWA90. It is also important to underline the existence of years with high HWN90 and low HWD90 or HWA90 (such as 1985, 1999, 1997 and 2009) as well as years with low HWN90 and high HWD90 or HWA90 (such as 1983, 1990, 2006 and 2010), revealing that more amplitude does not mean more duration or more number of HWs.

The temporal evolution present some trends in HW features that can be underlined, namely a significant increase of about 4 days per decade in HWD90 and 2000 °C per decade in HWA90 for the entire study period (1981–2010) and quite different tendencies for two sub-periods. Between 1981 and 1992 there is a smooth decreasing linear trend for HWN90 (−1.2 HW per decade) but a very pronounced growing linear trend in HWD90 (17 days per decade) and HWA90 (52,000 °C per decade). For the following sub-period (1993–2010), the three descriptors present an increase linear trend, much more significant for HWD90 (16 days per decade) and HWA90 (1850 °C per decade) but, less accentuated than for the first sub-period.

3.2. The role of HW on EW occurrence

HWs are clearly associated to the temporal and spatial distribution of EWs in Portugal. The analysis of the duration dates of EWs and HWs during the 1981–2010 period reveals that: (i) 97% of total number of EWs were active during HWs; (ii) 90% of the total number of EWs days were also HWs days; and (iii) 82% of the EWs had duration completely contained in the duration of an HW. About 45% of the total number of EWs occurred during just three HWs, namely 13 during the 28 July – 16 August 2003 HW, 7 in the 11–26 August 2005 HW and 6 during the 1–26 August 1991 HW. The others HWs associated with EWs just account for one or two wildfire events. It is also important to underline that 60 of the 62 EWs occurred during 29 (23%) of the 130 total number of observed HWs.

Besides the good agreement between the temporal distribution of EWs and HWs, it is also important to assess the spatial coherence between the location of EWs and spatial extent of HWs. Results reveal that 50 (83% of total) EWs occurred in the area affected by an HW, 3 (5%) in a short distance (<30 km) of this area and 9 (14%) at a distance >30 km. Analysis for the years with higher EW BA and (Figs. 7 and 8) disclose that the about nearly two thirds of these (40, 64.5% of total) EW occurred inside areas affected by HW and in or near regions where HW duration and amplitude were higher. This analysis illustrate the outstanding magnitude of 2003 and 1991 HWs in relation to the other hot spells which, in turn, helps to understand the location of the EWs in the region of higher HWA90 and HWD90, especially in 2003.

It should also be mentioned that, apparently, some EWs did not occur in regions affected by HWs. As will be explained in Section 4, these cases are also associated with the occurrence of hot weather events with T_{max} > P90 over a large area, that lasted several but less than the 6 consecutive days, which officially define the occurrence of an HW. It is also worth noting that these EWs occurs in regions previously affected by HWs (Fig. 8).

3.3. HWs in a future climate

Future HWs will occur in an overall warmer summer climate. In order to evaluate whether future HWs characteristics are also more extreme in a relative sense with respect to the warmer mean summer climate, we computed the average, the minimum and maximum value of HW number (HWN90), duration (HWD90), amplitude (HWA90), and frequency (HWF90), for 2021–2050, 2031–2060, 2041–2070, 2051–2080 and 2061–2090 periods (Table 1) in relation to the P90 computed for the correspond future period (Fig. 9). The ensemble mean of P90 difference computed for future and control climatological periods reveals an increasing trend in time with a SW-NE gradient in space. Results for RCP 4.5 ranges from 1 to 2 °C in 2021–2051 to 2–3 °C in 2061–2090 while for RCP 8.5 vary from 1 to 2 °C (in SW-NE) in 2021–2051 to 3–6 °C in 2061–2090.

HWN90 relative to the corresponding future periods are expected to increase on average by about 9 HWs every 30 years (2021–2090) for both RCP's. Furthermore, multi model average of HWD90 for 2021–

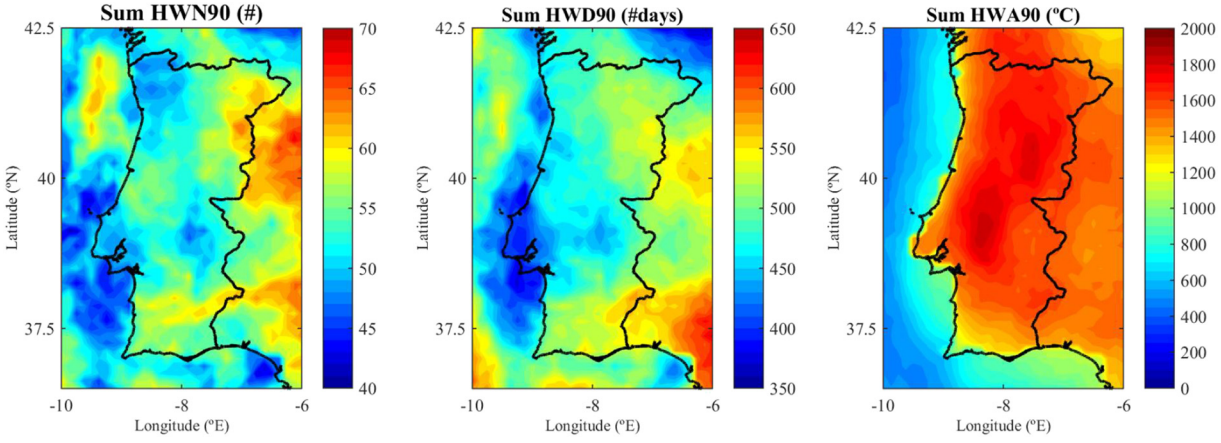

Fig. 4. Sum of the heat wave number (HWN90, left panel), duration (HWD90, central panel) and amplitude (HWA90, right panel) in each grid point of ERA-Interim reanalysis dataset (0.125° lon × 0.125° lat) spatial domain, for 30-year climatological period 1981–2010.

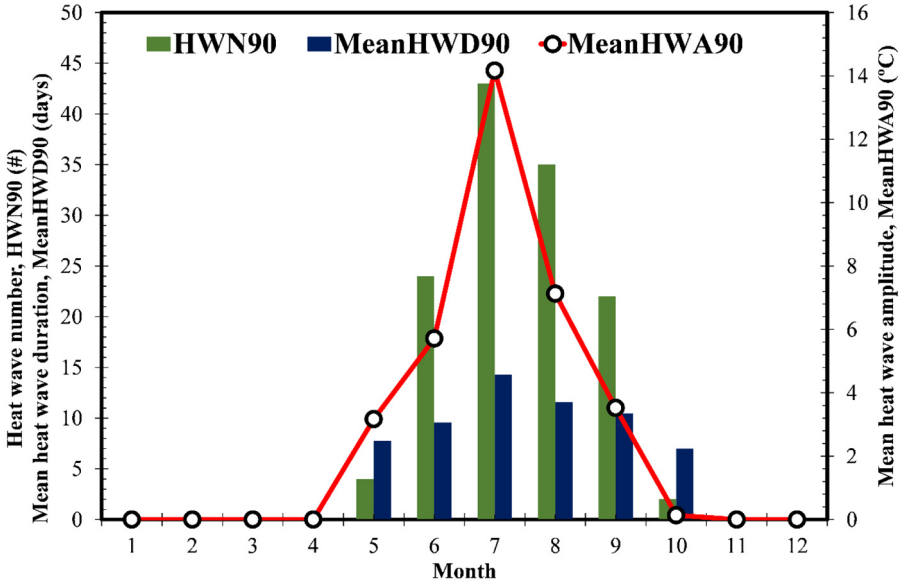

Fig. 5. Monthly distribution of heat wave number (HWN90), mean heat wave duration (MeanHWD90) and mean heat wave amplitude (MeanHWA90) for control period (1981–2010).

2090, reveals that simulated HWs are 6% (for RCP 4.5) and 17% (for RCP 8.5) longer than the ones between 1981 and 2010. In fact, multi model averages differences of HWD90 for the five future climate periods ranges between −2%–13% and (RCP 4.5) and 8%–25% (RCP 8.5). In addition it is also worth noting that average maximum HWD90 changes between 153 and 271 days (10–18%) for RCP 4.5 and between 212 and 622 days (14–41%) for RCP 8.5. For RCP 4.5, simulated HWs amplitude decreases 5% in the first 4 periods, and increases 5% on the last period. In RCP 8.5, HWA90 increases 15% between 2061 and 2090. HWF90 strongly increases in RCP 8.5, namely 8% in the first period, 25% between 2061 and 2090. In short, HWs will increase about 4% of frequency in each 30-year period in relation to the value obtained for the control period. Overall, this suggests that future HWs characteristics may also change beyond the effects of simple mean warming. However, it is unclear to what extent the strong trend within future period is part of the forced climate response or induced by inter-annual and decadal climate variability.

4. Discussion

First of all, we should acknowledge that biases of the reanalysis may affect the identification of extreme events when using this data as surrogates of observations; however, ERA-Interim seems to be the most advisable reanalysis product to the identification of some extreme events (Bedia Jiménez et al., 2012). In this respect, it is important to underline the good agreement between results obtained in this study with ERA-Interim dataset for 1981–2010 period and the maps published in the Iberian climate Atlas produced with data observed in a large set of weather stations, although for a slightly different (1971–2000) period (Couto et al., 2011). For example, spatial patterns of T_{max} statistical distribution's resistant and robust measures of Q2, P10 and higher percentiles (P90, P95 and P99), shown in Fig. 2, resemble quite well, respectively, the maximum air temperature annual, winter (December, January and February) and summer (June, July and August) average maps. Patterns of the sum of HWN90 and HWD90, presented in Fig. 4,

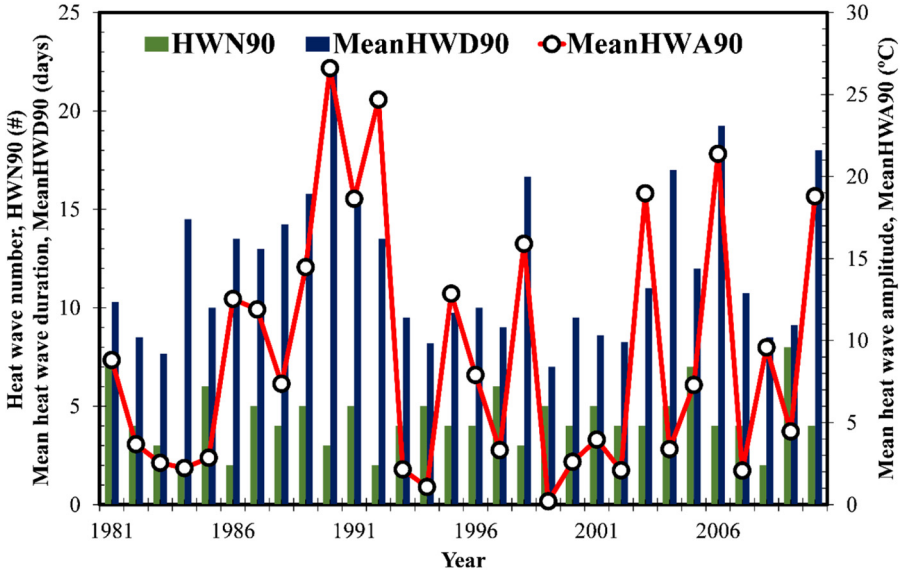

Fig. 6. Annual distribution of heat wave number (HWN90), mean heat wave duration (MeanHWD90) and mean heat wave amplitude (MeanHWA90), for control period (1981–2010).

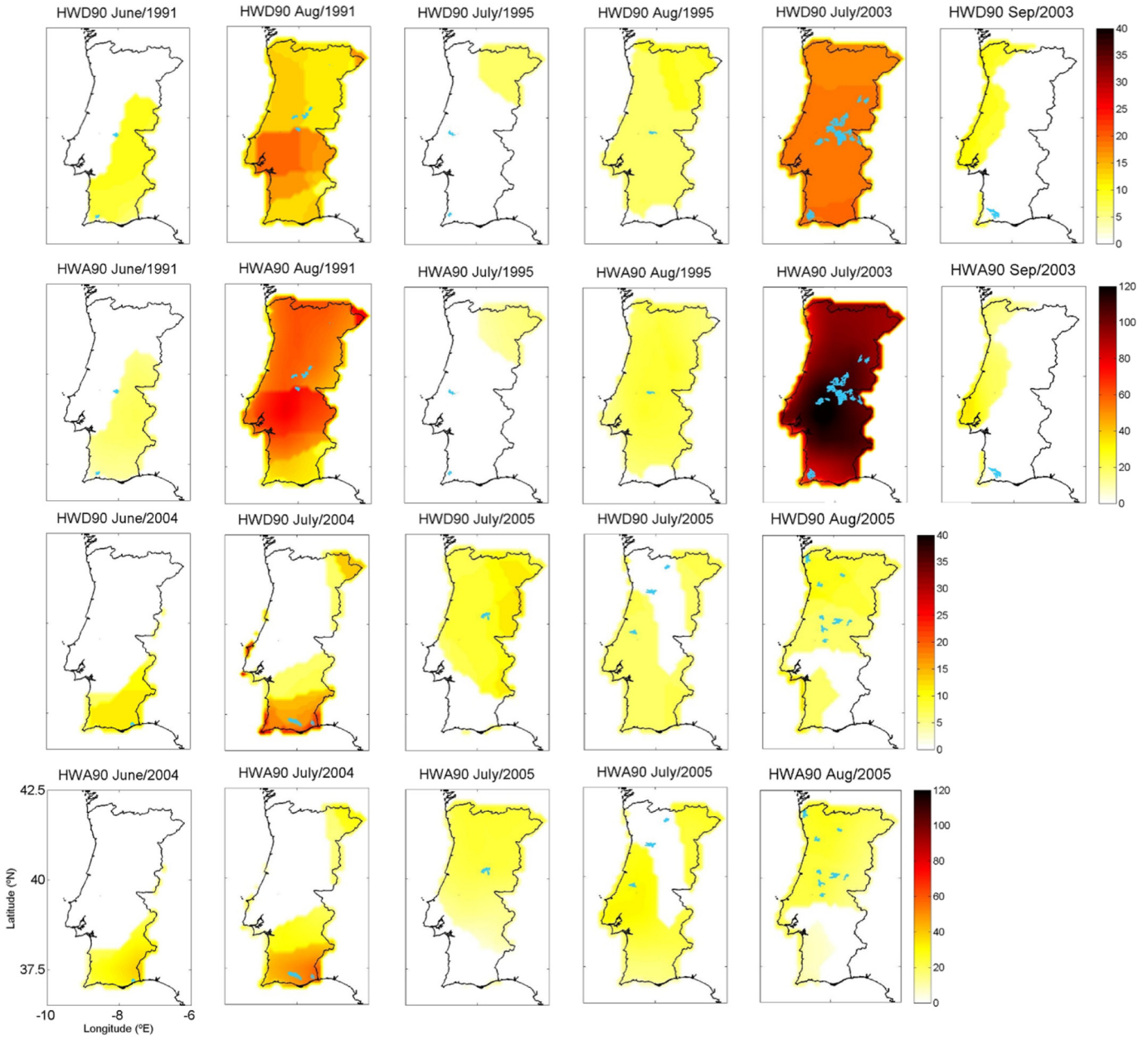

Fig. 7. Heat wave duration (HWD90) and amplitude (HWA90) for each heat wave associated to the occurrence of extreme wildfires (burnt area ≥ 5000 ha) in the years (1990, 1991, 1995, 2003, 2004 and 2005) with the largest burnt area and the number of extreme wildfires.

are well supported by the map of the average number of days with $T_{max} \geq 25$ °C, which present higher values (>110 days per year) in the northeast area and the highest values (>150 days per year) in inland southern Portugal. Despite the adequacy of the ERA-Interim data to identify and characterize extreme events of climatic elements had already been demonstrated in previous studies (e.g. Russo et al., 2014), these results confirm this capacity, in particular for T_{max}.

The monthly distribution of HWN90, mean HWD90 and mean HWA90 (Fig. 5) with higher values in the dry and hot semester, specifically during the summer months, is a consequence of the climatological normal of air temperature, not only in Portugal (Couto et al., 2011; Pereira et al., 2013) but also in other European countries (D'Ippoliti et al., 2010). In fact, the HW duration and amplitude tends to be higher in warmer conditions. For example, HWs are longer and more intense in southern US than in the Midwest or Northeast (Anderson and Bell, 2011).

The high inter-annual variability of HW aspects (Fig. 6) is characterized by three main features. First, the alternation between lower and higher values of HWD90 and HWA90, which can be interpreted in terms of the existence of years with extremely hot and dry summers, associated with persistent anticyclonic circulation, high sunshine, exceptionally few cyclonic days and low precipitation. These conditions, in particular extreme values of near-surface air temperature in mainland Portugal (Espírito Santo et al., 2014) and the occurrence of HWs with higher impacts in Portugal have been documented for extreme years of 1990 (Monteiro and Velho, 2014), 1991 (Dessai, 2002; Marto, 2005), 1998 (Stefanon et al., 2012), 2003 (Dasari et al., 2014; Rebetez et al., 2006, 2009), 2006 (Dasari et al., 2014; Monteiro et al., 2013) and 2010 (Barriopedro et al., 2011; Miralles et al., 2014). Second, some HWs characteristics appear to be uncorrelated, which means, for example, that higher number of events do not necessarily imply longer or more intense HWs. In fact, annual HWN90 is negatively correlated with both annual mean HW duration (−0.24) and amplitude (−0.31)

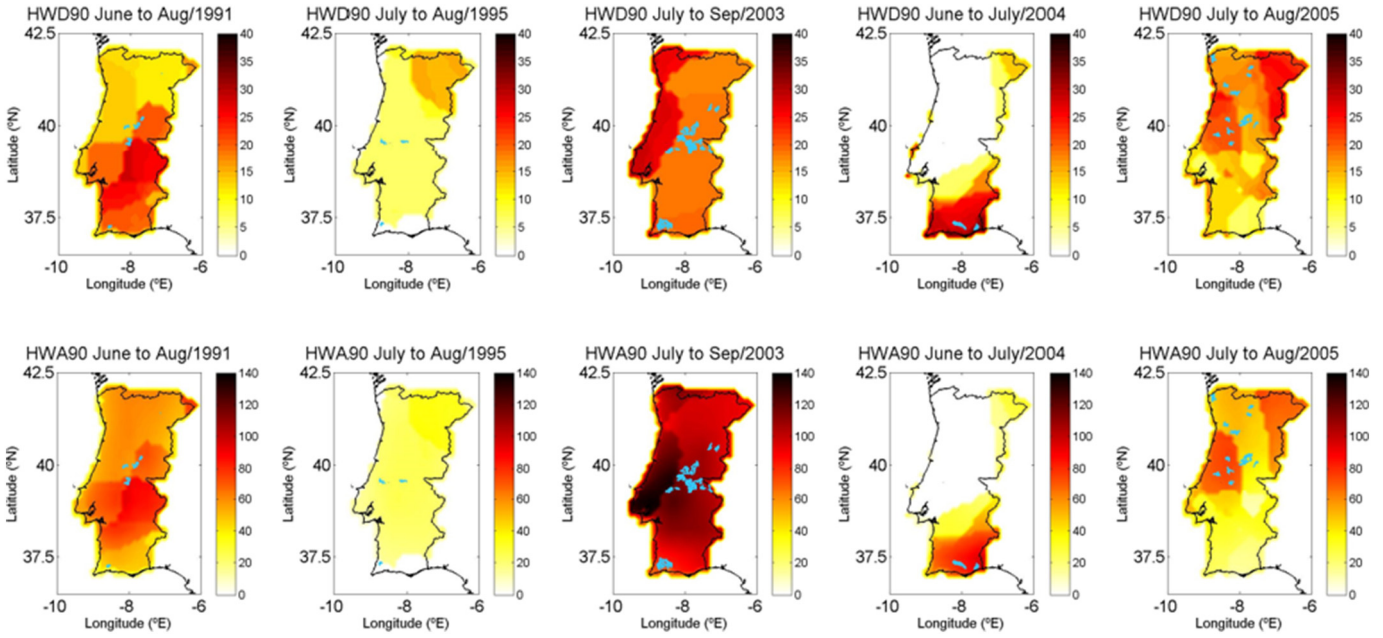

Fig. 8. Sum of heat wave duration (HWD90) and amplitude (HWA90) associated to the occurrence of extreme wildfires (burnt area ≥ 5000 ha) in the years (1990, 1991, 1995, 2003, 2004 and 2005) with the largest burnt area and the number of extreme wildfires.

while the Pearson product-moment correlation coefficient between HWD90 and HWA90 (0.73) reveal that these two variables are positively correlated which do not prevent the existence of years of high duration and low amplitude and vice-versa. This apparent contradiction has been reported for HW in other locations (Anderson and Bell, 2011; Russo et al., 2014) including different trends in HWs characteristics (Perkins and Alexander, 2013). In fact, this negative correlation can be explained by the fact that in some years HWs can be interrupted by cold air masses like cyclones and associated fronts, and northerly advections, which lead to shorter hot extreme events (Miralles et al., 2014). Typically it takes several days to build up an extreme HW due to drought, soil drying and accumulation of heat in the boundary layer and positive feedbacks between low-level atmospheric temperatures (Beniston, 2004; Miralles et al., 2014). Third, the increasing trends of HWD90 and HWA90 for the entire period and for the two consecutive sub-periods (1981–1992 and 1993–2010).

Trend analysis on meteorological variables and parameters computed with reanalysis data should be performed with extreme care because they may not represent true climate tendency due to the inability of the data assimilation system to correct instrumental and processing changes in the global observing system. The list of changes may be caused by the introduction of new types of data (e.g., satellite data), model differences (e.g., topographical differences and surface land schemes) and increased spatial coverage, (Bengtsson et al., 2004; Cai and Kalnay, 2005; You et al., 2010). However, it must be underlined that most significant changes occurred in the 1950s and in 1979 (before the study period) (Cai and Kalnay, 2005). The ERA-Interim dataset used in this study have suffered several bias treatments in global physically consistent framework, leading to a more consistent representation of climate signals in the reanalysis which support the use of this dataset for temperature trend assessment and to monitor climate change (Dee et al., 2011).

Della-Marta et al. (2007a, 2007b) found the largest, positives and statistical significant trends of European HWs between 1880 and 2005 over Iberian Peninsula. Espírito Santo et al. (2014) analysed the seasonal trends in indices of maximum and minimum temperature extremes,

Table 1
Relative changes in HW characteristics with respect to the corresponding future mean climate. Differences (Δ) between Heat wave number (HWN90, heat waves per year), Heat wave duration (HWD90, days), Heat wave amplitude (HWA), Heat wave frequency (HWF90, days per year) for 5 different/consecutive 30-year future climatological periods (namely, 2021–2050, 2031–2060, 2041–2070, 2050–2080 and 2061–2090), two representative concentration pathways (RCP 4.5 and RCP 8.5) and simulated by 3 pairs of GCM/RCM in relation to P90 computed for future periods.

		HWN90 (heat waves per period)		HWD90 (days)		HWA (°C)		HWF90 (days)	
Obs	1981–10	130		1524		1,086,506		0.139	
Mean ($\overline{\Delta}$), minimum (Δ_{min}) and maximum (Δ_{max}) difference		$\overline{\Delta}$	(Δ_{min}/Δ_{max})	$\overline{\Delta}$	(Δ_{min}/Δ_{max})	$\overline{\Delta}$	(Δ_{min}/Δ_{max})	$\overline{\Delta}$	(Δ_{min}/Δ_{max})
RCP4.5	2021–50	7	(−9/20)	−30	(−390/153)	−29,404	(−195,525/64,671)	−0.003	(−0.036/0.014)
	2031–60	11	(−4/20)	33	(−421/289)	−76,023	(−326,803/112,378)	0.003	(−0.039/0.027)
	2041–70	14	(7/20)	113	(−297/320)	−65,584	(−336,230/223,200)	0.010	(−0.027/0.029)
	2051–80	11	(6/17)	164	(−78/305)	−48,815	(−268,336/214,851)	0.015	(−0.007/0.028)
	2061–90	4	(−5/9)	197	(77/271)	51,445	(−42,422/234,903)	0.018	(0.007/0.025)
RCP8.5	2021–50	10	(−9/20)	116	(−13/212)	3597	(−19,091/45,990)	0.011	(−0.001/0.019)
	2031–60	8	(−14/23)	198	(143/260)	−22,219	(−108,164/29,025)	0.018	(0.013/0.024)
	2041–70	4	(−20/21)	280	(210/382)	7227	(−193,620/163,140)	0.026	(0.019/0.035)
	2051–80	9	(−12/27)	345	(265/462)	52,423	(−134,392/244,111)	0.032	(0.024/0.042)
	2061–90	12	(−5/21)	385	(234/622)	160,322	(−13,411/360,223)	0.035	(0.021/0.057)

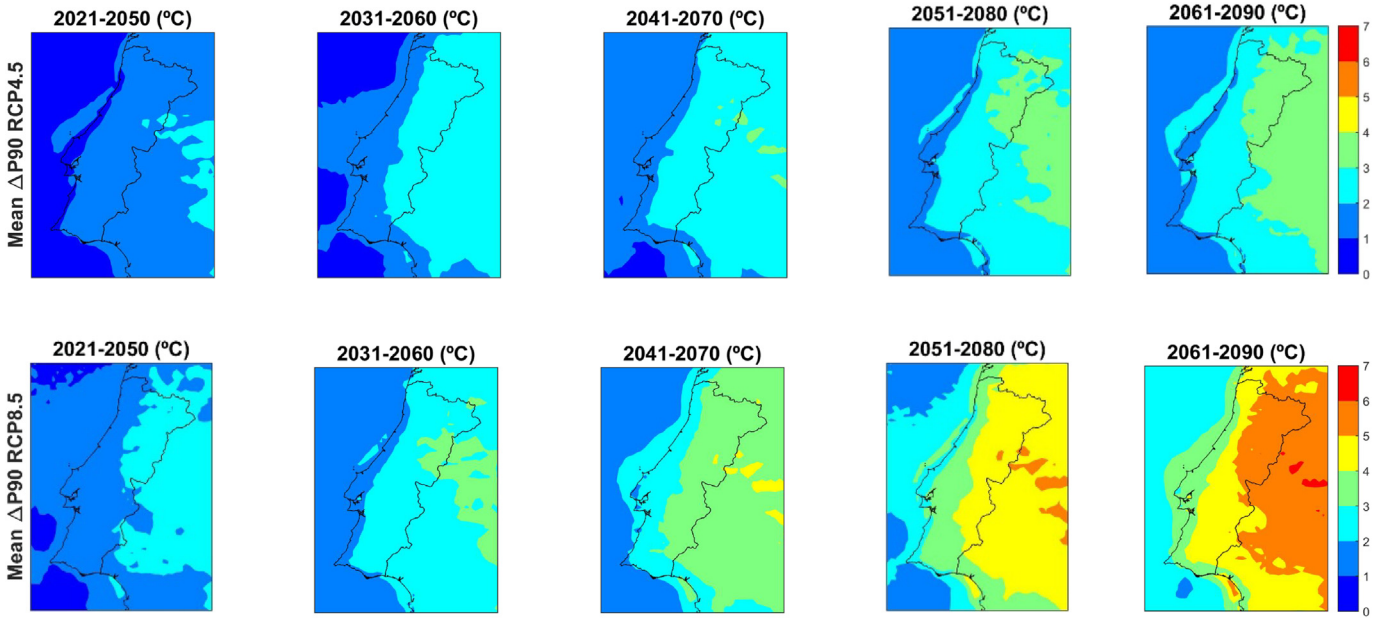

Fig. 9. Ensemble mean difference of P90 for future climatological periods in relation to control period. All changes are robust, i.e., concordant and significant.

based on surface air temperature, observed in 23 weather stations from 1941 to 2006, in continental Portugal. They identified a cooling (1945–1975) and a warming period (1976–2006) almost coincident with this study period. They also found positive trends in spring (defined as March, April and May) and summer (June, July and August) of the warming period for all HWD90 time series, 13 (5) statistical significant at 5% level, which correspond to an average of 1.42 days per decade (1.53 days per decade).

These results are in line with our findings for HWD90, computed from March to October, for both sub-periods (1.71 days per decade for 1981–1992 and 1.56 days per decade for 1993–2010). The time series with statistical significant increasing trends (in spring and summer) corresponds to *Montalegre*, *Bragança*, *Penhas Douradas*, *Elvas*, *Setúbal*, *Amareleja*, *Beja* and *Sagres* weather stations (Fig. 1), precisely located in the regions where most EWs (Fig. 3) occurred.

To understand other aspects of the variability of HW characteristics, namely the trends in inter-annual variability, it is important to take into account that Portugal's climate is largely determined by the frequent passage of synoptic extratropical weather systems, within the predominantly mid-latitude zonal atmospheric circulation from west to east, in association to the jet stream (Santos et al., 2013; Sousa et al., 2017). The usual alternation between periods of hot and dry days and rainy and cold days associated with extra-tropical cyclones has a length ranging from weeks to months but can be interrupted by the occurrence of blocking systems or subtropical ridges (Sousa et al., 2016, 2017).

It is important to note that blockings are large–scale high pressure systems with quasi-stationary anticyclonic circulation with the ability to interrupt the prevailing westerly winds in the mid-to-high latitudes and life time of few days to several weeks (Barriopedro et al., 2011). The heavy tail statistical distribution of the duration of Northern Hemisphere summer blocking episodes for the period 1950–2012 ranges from 5 to almost 30 days (Sousa, 2017) which helps to understand the platykurtic character of inter-annual distribution of mean HWD90 as well as the monthly mean range between 7 and 14 days (Fig. 5). On the other hand, ridges are a northward extension of the sub-tropical high pressure belt, without the ability to split the extratropical Jetstream into two branches but to reinforce and push northwards the local westerly flow, i.e., ridges do not require Rossby wave-breaking occurrence as in high latitude blocks (Sousa, 2017).

In general, HWs in western Europe are associated with specific atmospheric circulation patterns, characterized by the existence of these semi-stationary high-latitude blocking systems or sub-tropical ridges (Sousa et al., 2017). For example, it is a matter of definition if the outstanding HW that affected western and central Europe in 2003 was associated to a typical atmospheric blocking (Trigo et al., 2005) or to a northward expansion of the subtropical high (García-Herrera et al., 2010). As mentioned above, blocks and ridges are important components of intra seasonal and inter-annual variabilities at mid-latitudes because of their effects on local precipitation and temperature, yet regional synoptic conditions, involved processes and local impacts depend on the blocking system's location and season of occurrence (e.g., Garcia-Herrera et al., 2007 and Sousa et al., 2016).

Weather in Portugal is particularly affected by Euro-Atlantic blocking systems which have the ability to deflect storm tracks towards north or south, decreasing or increasing precipitation in those areas, as well as clear sky conditions and dry periods (Trigo et al., 2004). Seasonal impacts of blocks and ridges on European air temperature at continental and regional scales are described in terms of horizontal and vertical advection as well as adiabatic heating in Sousa et al. (2017). According to this study, the atmospheric circulation during winter blocks tends to favour the advection of cold and dry air from northern latitudes to southern Europe, including Portugal, promoting drought and the occurrence of cold spells. On the other hand, ridges contribute to anomalously warm conditions by advection of Atlantic air masses and reduced long wave radiation cooling. During summer, both blocking and ridges patterns tend to contribute to above average air temperatures, more pronounced for T_{max} than for minimum air temperature (T_{min}) and, consequently, to higher frequency of extremely warm days driven by radiative heating associated to cloudless conditions and enhanced insolation hours, especially in central Europe, but only ridges lead to positive temperature anomalies in Mediterranean countries. The probability density function of T_{max} for summer during both blocks and ridges present a noticeable shift towards higher values, more significant for ridges than for blocks, and in T_{max} than in T_{min}, with a pronounced rise in 90th percentile of T_{max}, in frequency of extremely hot days in almost all regions and in number of days with $T_{max} > 35$ °C in Iberian Peninsula (Sousa et al., 2017).

The role of blocks and ridges on HW occurrence helps to understand, at least partially, the inter-annual variability of HW characteristics not only for recent past but also for future climate conditions. In fact, the increasing trends of HWD90 and HWA90 in 1981–1992 and 1993–2010 periods are also observed by Barnes et al. (2014) for blocking

frequencies in North Atlantic (60 W–0 W) during summer (June, July and August), using four different reanalysis datasets (ERA-Interim, NCEP/NCAR, MERRA and NCEP2) as well as two distinct blocking indices. The frequency of sub-tropical ridges and high-latitude blockings over the Atlantic (30 W–0 W) and European (0 E–30 E) sectors was recently analysed by (Sousa, 2017) using NCEP/NCAR reanalysis (1950–2012), an automatic blocking detection method (Barriopedro et al., 2006) and a novel ridge detection scheme (Sousa et al., 2017), also disclosing similar increasing trends for the frequency of ridges during summer and blocks in winter. It is important to further mention that many studies have shown that most of the increase in HWs simply follows the mean summer warming over longer period (Beniston, 2004; Della-Marta et al., 2007b), climate models mean warming accounts for almost the whole increase in HWs (Ballester et al., 2010; Della-Marta et al., 2007a; Fischer and Schär, 2010; Lustenberger et al., 2014), as well as there is no clear long-term trend in blocking in many places.

Several studies have focused on the role of pre-conditioning drought conditions and the amplifying effect of land-atmosphere feedbacks in the occurrence and amplitude of HW (Miralles et al., 2014). In fact, Stéfanon et al. (2014) concluded that the majority of recent summer HW events in Europe were preceded by significant precipitation deficit in previous months which lead to lower soil moisture, less evapotranspiration, reduced latent heat cooling and higher sensible heat flux which amplify extreme summer air temperatures. Additionally, Fischer et al. (2007) performed simulations with coupled land-surface models and suggested the increase of surface net radiation, enhanced evaporation during spring, HW duration, number of hot summer days in 50–80% and, mainly, on daily T_{max} during HW. Miralles et al. (2014) analysed the mega HW of 2003 and 2010 in Europe with observed and simulated data and revealed that extreme air temperatures were due to combined soil desiccation and atmospheric heat accumulation as a result of land–atmosphere feedbacks induced by persistent atmospheric pressure patterns. Therefore, it is also worth noting that drought has been more frequent in southern Europe, namely in Iberian Peninsula and in the later decades of the 20th century (Sousa et al., 2017; Spinoni et al., 2015) because it helps to explain the increasing trends of HWs characteristics during our study period.

Factors that favouring the occurrence and development of HW are also main drivers of wildfires. As mentioned previously, the inter-annual variability of fire activity result from climatic conditions in the pre-fire season, namely a period of less precipitation – drought – somewhere between late winter and early summer, and the occurrence of intense hot spells – heat waves – during the summer fire season (Bedia et al., 2015; Ferreira-Leite et al., 2017; Jolly et al., 2015; Pereira et al., 2014). In this sense, it is easy to envisage the coincidence between the timing and geographic location of the occurrence of EWs (Figs. 7 and 8) and the spatial and temporal extent of HW. It would already be important to verify if each of the 62 EWs occurred during one of the 130 HWs, which would mean, 62/130 = 0.48 EW/HW. However, it turns out that 60 EWs occur only during 29 HWs, which means a four times higher ratio of 2.1 EW/HW. This is a consequence of a significant number of EWs occurred during the same HW, especially during very long and intense HW of 1991, 2003 and 2005. Moreover, in relation to HW without EW, the HW with EW are 3% longer, 16% larger and 25% more intense The 2 EWs that did not occur simultaneously with a HW, occur immediately after a set of several HWs (Fig. 12). The EW of 2001 start in beginning of September after 3 HWs; the first one in May, the second in June and the third in August. The EW of 2005 occur in the middle of September (17–24), after 5 HWs between June and September. It should also be mentioned that, apparently, some EWs did not occur in regions affected by HW. The EW in the SW region of Portugal during September 2003 (Fig. 7), occurred with $T_{max} > P90$ for a few days but less than the 6 consecutive days that define the occurrence of an HW. The same argument serves as an explanation for the wildfires occurred in the North region during the year of 2005. These results seem to suggest the adoption of a minimum period of <6 days to define an HW in the future, as it is already being used in Australia where there are many short HW (Boschat et al., 2015; Perkins et al., 2012).

The latest simulations of the maximum temperature with corrected bias produced by GCM/RCM model pairs for RCP 4.5 and RCP 8.5 allowed us to assess the potential impacts of climate change on HW. The use of physical downscaling of GCM simulations with RCM is justified by the need to include local and regional effects, such as coastlines, topography, vegetation water bodies on the simulation of local climate (Dasari et al., 2014). It is also important to underline the use of bias corrected simulations for the future with DBS method chosen for this study, which seems to be able to reproduce well some aspects of T_{max} distribution and derived indices, such as the mean of the >90th percentile spell length (Maraun et al., 2017).

Obtained simulations with T_{max} for RCP 4.5 and RCP 8.5, suggest that: (i) P90 will increase significantly for all future climatological periods and both scenarios (Fig. 9); (ii) HW computed in relation future P90, will increase in number, amplitude and mostly in duration and frequency (Table 1); and, (iii) in relation to control period, changes in HW duration and amplitude are, in general, significant and robust in entire Continental Portugal territory, in all periods for RCP 8.5 but mainly after 2051–2061 for RCP 4.5 (Figs. 10 and 11). Although, to the best of our knowledge, there are no other studies of the projection of HWs to future climate scenarios specifically for Portugal, the findings of previous related studies allow us to validate our results obtained here.

Jacob et al. (2014) computed the projected changes of HW number in Europe during May–September for RCP 4.5 and RCP 8.5, using two different HW definitions, EURO-CORDEX ensemble simulations for two future periods (2021–2050 and 2071–2100) in relation to 1971–2000 control period. They obtained statistical significant and robust increases, smaller for RCP 4.5 than for RCP 8.5, more pronounced towards the end of the century as well as spatial distribution and magnitude similar to our results. Russo et al. (2015) used a magnitude index and ten EURO-CORDEX regional climate projections for 2020–2040 period to estimate HW's magnitude and show that the probability to have an extreme HW in Europe in that study period is higher for RCP 8.5 than RCP 4.5. Andrade et al. (2014) assess GCM/RCM multi-model chains' projections of air temperature extremes, including seasonal mean T_{max}, P90 and number of days with temperature above P90 (NDTX90p), for 2041–2070 in Portugal, and obtain a NDTX90p spatial pattern with higher values in the interior (NE and SE) well matched with our findings for future climate scenarios.

5. Conclusions

This study aimed to identify and characterize the occurrence and main features of heat waves in recent history, their impacts on the occurrence of extreme fires (burnt area ≥ 5000 ha) and expected variations in future climate change scenarios which, to our knowledge, had never been done for Portugal. Main findings can be summarized as follows. A total of 130 heat waves occurred in mainland Portugal between 1981 and 2010, exclusively during the dryer and hotter semester (between May and October) but particularly concentrated (60% of total number of heat waves) in July (33%) and August (27%). The leptokurtic distribution of monthly mean heat wave amplitude is very similar but intra-annual variability of mean heat wave duration is more homogeneous during the warm and dry semester. During the reference period, the annual number, mean duration and mean amplitude of the heat waves show high inter-annual variability. Increasing trends of HW characteristics are associated with a general mean warming trend during the entire study period, and in the two sub periods (1981–1992 and 1993–2010), with tendencies in the frequency of high-latitude blocking systems and sub-tropical ridges affecting mainland Portugal. Regions with higher number of heat waves were, by this order, the NE quarter, the southernmost region and, to a lesser extent and magnitude, the central western coastal region between, but out of, the metropolitan areas

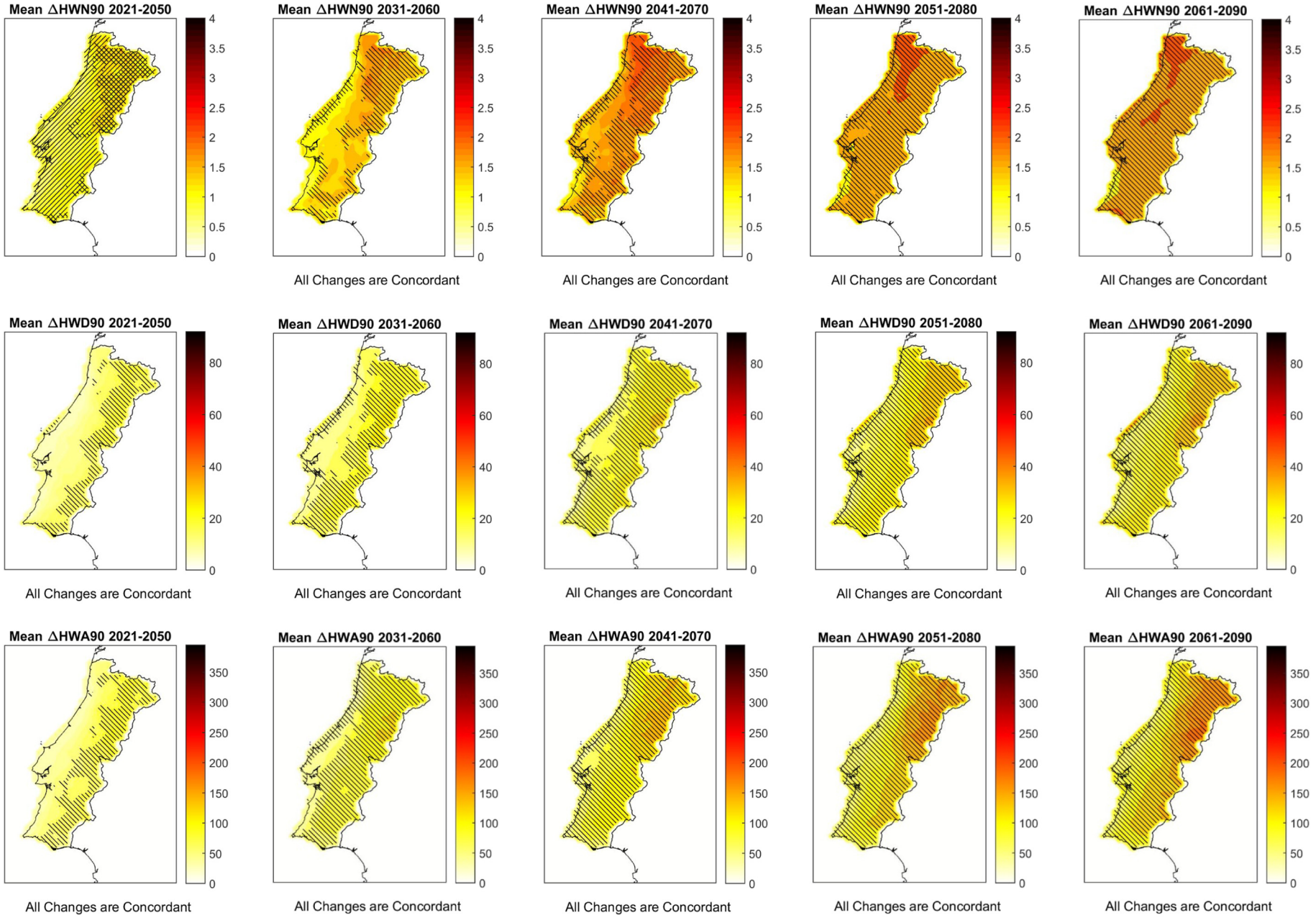

Fig. 10. Changes of heat wave mean number (HWN90), duration (HWD90) and amplitude (HWA90) for five future climatological periods of RCP4.5 in relation to control period 90th percentile (P90). Hatching: / concordant; \ significant.

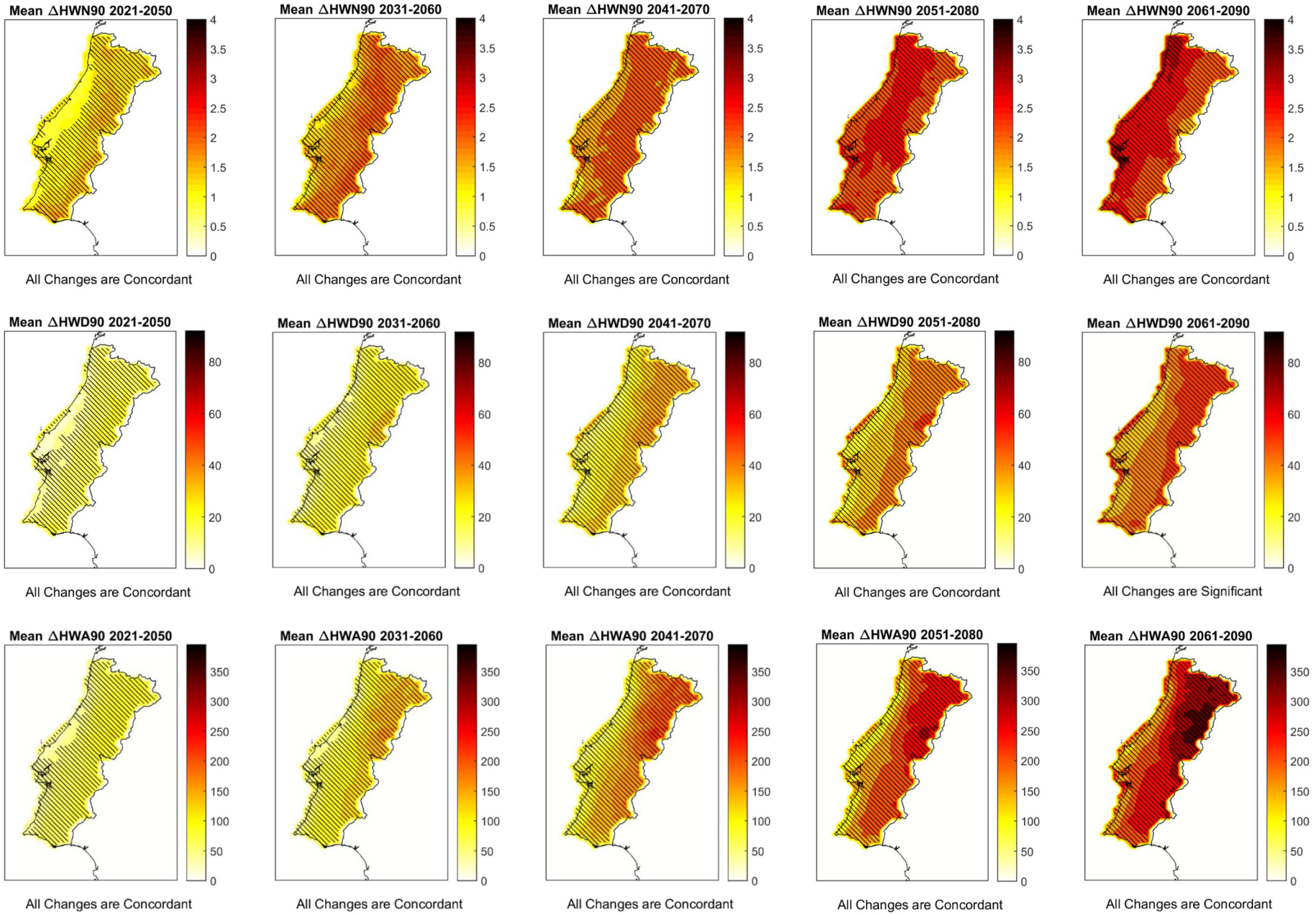

Fig. 11. Changes of heat wave mean number (HWN90), duration (HWD90) and amplitude (HWA90) for five future climatological periods of RCP8.5 in relation to control period 90th percentile (P90). Hatching: / concordant; \ significant.

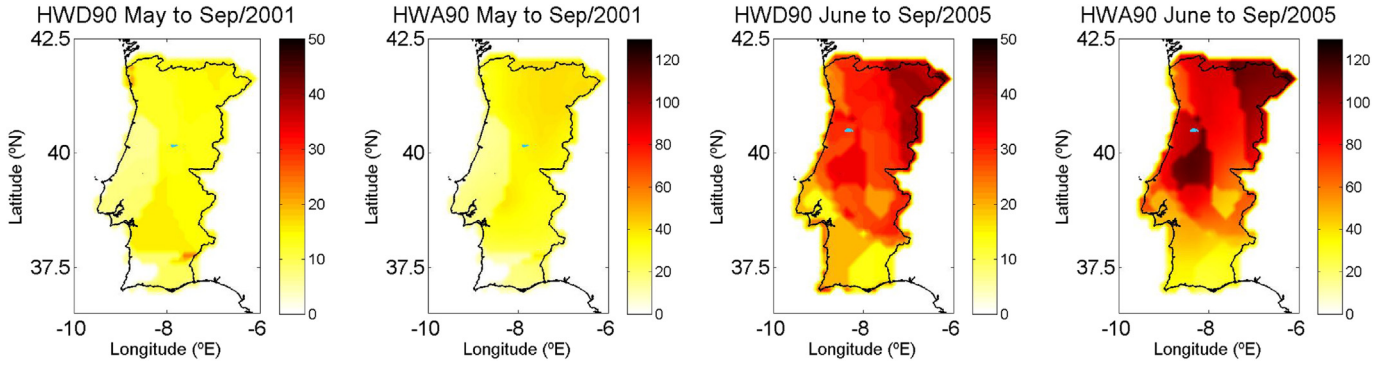

Fig. 12. Sum of heat wave duration (HWD90) and amplitude (HWA90) occurred before the extreme wildfires of September 2001 (left panels) and September 2005 (right panels). Extreme wildfires are also represented (light blue). (For interpretation of the references to colour in this figure legend, the reader is referred to the web version of this article.)

of Porto and Lisbon. Spatial pattern of total heat wave duration is similar but higher values are confined to the NE and South regions, while heat wave amplitudes show higher values in the SW-NE direction over central Portugal. This is precisely the region where most of the extreme wildfires occurred in modern time. Detailed analysis performed on the time and location of extreme wildfires in the study period allows to conclude that all these extreme events occurred during (96.8%) or immediately after (3.2%) several long and intense heat waves, precisely in the regions where these warm events were lengthier and vivid. Climate models project that maximum air temperature 90th percentile for both future climate scenarios (RCP 4.5 and RCP 8.5) are much higher (about 3–6 °C towards the end of the century, respectively for RCP 4.5 and RCP 8.5) than for current climate conditions. Even in a relative sense with respect to the future warmer summer climate heat waves are projected to increase in number, duration and amplitude, although this increase is more significant for RCP 8.5 than for RCP 4.5 scenario and for the 30-year periods near the late 21st century.

These conclusions are important because they provide a perspective of the heat wave regime with respect to future conditions, i.e., as if identified and characterized in the future, taking into account future P90 changes. However, the comparison between the future and current regime is facilitated if the heat waves are identified in relation to the P90 computed for the reference period. In this case, there is a generalized and robust increase in the number, duration and amplitude of the heat waves for the future climate. Changes in heat waves' duration and amplitude are expected to be higher in the interior, especially the northeast region. Projected changes in heat wave number for RCP 4.5 are higher in central north during the entire future study periods while for RCP 8.5 are higher in the interior and central north, respectively until mid-century and at the end of the 21st century. These changes tend to be more concordant, significant and robust for RCP 8.5 than for RCP 4.5 and to the end of the century.

The overall significance of the findings is also based on the use of an ensemble of bias corrected data simulated by state-of-the art pairs of global and regional climate models, to the fact that results were obtained for a high spatial resolution grid, over entire continental Portugal territory and for climatological periods of 30-years, not only for recent past but also for future climate conditions.

Heat waves, their characteristics, impacts and, consequently, the findings of this study are dependent on the definition used to identify these extreme climatic events. Since one of the objectives of the study was to relate the occurrence of heat waves and extreme wildfires we adopted the definition proposed by Fischer and Schär (2010). The use of another definition will eventually lead to different results but we believe that the adopted definition is the most suitable for the most important impacts of heat waves in Portugal, namely for wildfires.

Finally, the findings of this study can be very useful for the definition of adaptation and mitigation strategies for the impacts of heat waves, namely on human health and wildfires. A significant step in reducing the disaster risk of extreme weather or climate event is to minimize the vulnerability and exposure to current climate variability (IPCC, 2014). Obtained spatial and temporal patterns of heat waves' characteristics allow to identify the regions more affected and the periods (months, years and 30-year periods) of greater frequency of these events, not only in recent times but also for future climate scenarios. Furthermore, maximum air temperature is well simulated by global and regional atmospheric models which means that space-time occurrence of heat waves can be predicted with high confidence level. This high value information can be used for implementing warning systems, to help people to reduce exposure by predicting possible health outcomes, identifying triggers of effective and timely response plans for vulnerable populations, communicating risks and prevention responses (IPCC, 2014), namely to institutions responsible for forest and fire management to plan activities, concentrate and prepare firefighting resources and at times and in places affected by heat waves.

Acknowledgements

This work was prepared in the frame of project FIREXTR - Prevent and prepare society for extreme fire events: the challenge of seeing the “forest” and not just the “trees”, co-financed by the European Regional Development Fund (ERDF) through the COMPETE 2020 - Operational Program Competitiveness and Internationalization (POCI Ref: 16702) and national funds by FCT-Portuguese Foundation for Science and Technology (FCT Ref: PTDC/ATPGEO/0462/2014). The study was also supported by: i) Project Interact - Integrative Research in Environment, Agro-Chain and Technology, NORTE-01-0145-FEDER-000017, research line BEST, co-funded by FEDER/NORTE 2020; and, ii) European Investment Funds by FEDER/COMPETE/POCI– Operational Competitiveness and Internationalization Programme, under Project POCI-01-0145-FEDER-006958 and National Funds by FCT - Portuguese Foundation for Science and Technology, under the project UID/AGR/04033/2013. We are especially grateful to ICNF for providing the fire data and to João Pereira for the final spelling and grammar review of the manuscript.

References

Anderson, G.B., Bell, M.L., 2011. Heat waves in the United States: mortality risk during heat waves and effect modification by heat wave characteristics in 43 US communities. Environ. Health Perspect. 119, 210.

Andrade, C., Fraga, H., Santos, J.A., 2014. Climate change multi-model projections for temperature extremes in Portugal. Atmos. Sci. Lett. 15, 149–156.

Bador, M., Terray, L., Boe, J., Somot, S., Alias, A., Gibelin, A.-L., Dubuisson, B., 2017. Future summer mega-heatwave and record-breaking temperatures in a warmer France climate. Environ. Res. Lett. 12, 1–12.

Ballester, J., Rodó, X., Giorgi, F., 2010. Future changes in Central Europe heat waves expected to mostly follow summer mean warming. Clim. Dyn. 35, 1191–1205.

Barbero, R., Abatzoglou, J.T., Kolden, C.A., Hegewisch, K.C., Larkin, N.K., Podschwit, H., 2015. Multi-scalar influence of weather and climate on very large-fires in the eastern United States. Int. J. Climatol. 35, 2180–2186.

Barnes, E.A., Dunn-Sigouin, E., Masato, G., Woollings, T., 2014. Exploring recent trends in northern hemisphere blocking. Geophys. Res. Lett. 41, 638–644.
Barriopedro, D., García-Herrera, R., Lupo, A.R., Hernández, E., 2006. A climatology of northern hemisphere blocking. J. Clim. 19, 1042–1063.
Barriopedro, D., Fischer, E.M., Luterbacher, J., Trigo, R.M., García-Herrera, R., 2011. The hot summer of 2010: redrawing the temperature record map of Europe. Science 332, 220–224.
Bedia Jiménez, J., Herrera García, S., Gutiérrez Llorente, J.M., Zavala Espiñeira, G., Rodríguez Urbieta, T.I., Moreno Rodríguez, J.M., 2012. Sensitivity of Fire Weather Index to Different Reanalysis Products in the Iberian Peninsula.
Bedia, J., Herrera, S., Gutiérrez, J.M., Benali, A., Brands, S., Mota, B., Moreno, J.M., 2015. Global patterns in the sensitivity of burned area to fire-weather: implications for climate change. Agric. For. Meteorol. 214, 369–379.
Bengtsson, L., Hagemann, S., Hodges, K.I., 2004. Can climate trends be calculated from reanalysis data? J. Geophys. Res. Atmos. 109.
Beniston, M., 2004. The 2003 heat wave in Europe: a shape of things to come? An analysis based on Swiss climatological data and model simulations. Geophys. Res. Lett. 31.
Blarquez, O., Ali, A.A., Girardin, M.P., Grondin, P., Fréchette, B., Bergeron, Y., Hély, C., 2015. Regional paleofire regimes affected by non-uniform climate, vegetation and human drivers. Sci. Rep. 5, 13356.
Boschat, G., Pezza, A., Simmonds, I., Perkins, S., Cowan, T., Purich, A., 2015. Large scale and sub-regional connections in the lead up to summer heat wave and extreme rainfall events in eastern Australia. Clim. Dyn. 44, 1823–1840.
Cai, M., Kalnay, E., 2005. Can reanalysis have anthropogenic climate trends without model forcing? J. Clim. 18, 1844–1849.
Chung, U., Gbegbelegbe, S., Shiferaw, B., Robertson, R., Yun, J.I., Tesfaye, K., Hoogenboom, G., Sonder, K., 2014. Modeling the effect of a heat wave on maize production in the USA and its implications on food security in the developing world. Weather Clim. Extrem. 5, 67–77.
COGECA, C, 2003. Assessment of the impact of the heat wave and drought of the summer 2003 on agriculture and forestry. Comm. Agric. Organ. Eur. Union Gen. Comm. Agric. Coop. Eur. Union Bruss.. 15
Costa, L., Thonicke, K., Poulter, B., Badeck, F.-W., 2011. Sensitivity of Portuguese forest fires to climatic, human, and landscape variables: subnational differences between fire drivers in extreme fire years and decadal averages. Reg. Environ. Chang. 11, 543–551.
Couto, M.A., Sánchez, G., Tavares, C.D., Barceló, A.M., Nunes, L.F., Herráez, C.F., Pires, V., Marques, J., Mendes, L., Chazarra, A., 2011. Atlas Climático Ibérico. Inst. Meteorol. Port. Agencia Estatal Meteorol. Minist. Medio Ambiente Medio Rural Mar. Madr..
Cowan, T., Purich, A., Perkins, S., Pezza, A., Boschat, G., Sadler, K., 2014. More frequent, longer, and hotter heat waves for Australia in the twenty-first century. J. Clim. 27, 5851–5871.
Dasari, H.P., Pozo, I., Ferri-Yáñez, F., Araújo, M.B., 2014. A regional climate study of heat waves over the Iberian peninsula. Atmos. Clim. Sci. 4, 841.
De Bono, A., Peduzzi, P., Kluser, S., Giuliani, G., 2004. Impacts of Summer 2003 Heat Wave in Europe.
Dee, D.P., Uppala, S.M., Simmons, A.J., Berrisford, P., Poli, P., Kobayashi, S., Andrae, U., Balmaseda, M.A., Balsamo, G., Bauer, P., 2011. The ERA-interim reanalysis: configuration and performance of the data assimilation system. Q. J. R. Meteorol. Soc. 137, 553–597.
Della-Marta, P.M., Haylock, M.R., Luterbacher, J., Wanner, H., 2007a. Doubled length of western European summer heat waves since 1880. J. Geophys. Res. Atmos. 112.
Della-Marta, P.M., Luterbacher, J., von Weissenfluh, H., Xoplaki, E., Brunet, M., Wanner, H., 2007b. Summer heat waves over western Europe 1880–2003, their relationship to large-scale forcings and predictability. Clim. Dyn. 29, 251–275.
Dessai, S., 2002. Heat stress and mortality in Lisbon part I. Model construction and validation. Int. J. Biometeorol. 47, 6–12.
DGS, 2013. Relatório da onda de calor de 23/06 a 14/07 de 2013 em Portugal continental.
Dhainaut, J.-F., Claessens, Y.-E., Ginsburg, C., Riou, B., 2004. Unprecedented heat-related deaths during the 2003 heat wave in Paris: consequences on emergency departments. Crit. Care 8, 1.
D'Ippoliti, D., Michelozzi, P., Marino, C., De'Donato, F., Menne, B., Katsouyanni, K., Kirchmayer, U., Analitis, A., Medina-Ramón, M., Paldy, A., 2010. The impact of heat waves on mortality in 9 European cities: results from the EuroHEAT project. Environ. Health 9, 37.
Duchez, A., Frajka-Williams, E., Josey, S.A., Evans, D.G., Grist, J.P., Marsh, R., McCarthy, G.D., Sinha, B., Berry, D.I., Hirschi, J.J., 2016. Drivers of exceptionally cold North Atlantic Ocean temperatures and their link to the 2015 European heat wave. Environ. Res. Lett. 11, 074004.
Espírito Santo, F., de Lima, M.I.P., Ramos, A.M., Trigo, R.M., 2014. Trends in seasonal surface air temperature in mainland Portugal, since 1941. Int. J. Climatol. 34, 1814–1837.
Ferreira-Leite, F., Ganho, N., Bento-Gonçalves, A., Botelho, F., 2017. Iberian atmosferic dynamics and large forest fires in mainland Portugal. Agric. For. Meteorol. 247, 551–559.
Fischer, E.M., Schär, C., 2010. Consistent geographical patterns of changes in high-impact European heatwaves. Nat. Geosci. 3, 398–403.
Fischer, E.M., Seneviratne, S.I., Lüthi, D., Schär, C., 2007. Contribution of land-atmosphere coupling to recent European summer heat waves. Geophys. Res. Lett. 34.
Flannigan, M.D., Wotton, B.M., Marshall, G.A., de Groot, W.J., Johnston, J., Jurko, N., Cantin, A.S., 2016. Fuel moisture sensitivity to temperature and precipitation: climate change implications. Clim. Chang. 134, 59–71.
Fouillet, A., Rey, G., Laurent, F., Pavillon, G., Bellec, S., Guihenneuc-Jouyaux, C., Clavel, J., Jougla, E., Hémon, D., 2006. Excess mortality related to the August 2003 heat wave in France. Int. Arch. Occup. Environ. Health 80, 16–24.
Garcia-Herrera, R., Hernández, E., Barriopedro, D., Paredes, D., Trigo, R.M., Trigo, I.F., Mendes, M.A., 2007. The outstanding 2004/05 drought in the Iberian peninsula: associated atmospheric circulation. J. Hydrometeorol. 8, 483–498.
García-Herrera, R., Díaz, J., Trigo, R.M., Luterbacher, J., Fischer, E.M., 2010. A review of the European summer heat wave of 2003. Crit. Rev. Environ. Sci. Technol. 40, 267–306.
Gehrig, R., 2006. The influence of the hot and dry summer 2003 on the pollen season in Switzerland. Aerobiologia 22, 27–34.
Gouveia, C.M., Bistinas, I., Liberato, M.L., Bastos, A., Koutsias, N., Trigo, R., 2016. The outstanding synergy between drought, heatwaves and fuel on the 2007 southern Greece exceptional fire season. Agric. For. Meteorol. 218, 135–145.
Gronlund, C.J., Zanobetti, A., Schwartz, J.D., Wellenius, G.A., O'Neill, M.S., 2014. Heat, heat waves, and hospital admissions among the elderly in the United States, 1992–2006. Environ. Health Perspect. 122, 1187.
Gruber, S., Hoelzle, M., Haeberli, W., 2004. Permafrost thaw and destabilization of alpine rock walls in the hot summer of 2003. Geophys. Res. Lett. 31.
Haeberli, W., Paul, F., Gruber, S., Hoelzle, M., Kääb, A., Machguth, H., Noetzli, J., Rothenbühler, C., 2004. Effects of the extreme Summer 2003 on glaciers and permafrost in the Alps–first impressions and estimations. Geophysical Research Abstracts, p. 03063.
Hernandez, C., Drobinski, P., Turquety, S., Dupuy, J.-L., 2015. Size of wildfires in the Euro-Mediterranean region: observations and theoretical analysis. Nat. Hazards Earth Syst. Sci. 15, 1331–1341.
IPCC, 2014. In: Core Writing Team, Pachauri, R.K., Meyer, L.A. (Eds.), Climate Change 2014: Synthesis Report. Contribution of Working Groups I, II and III to the Fifth Assessment Report of the Intergovernmental Panel on Climate Change. IPCC 151.
Jacob, D., Petersen, J., Eggert, B., Alias, A., Christensen, O.B., Bouwer, L.M., Braun, A., Colette, A., Déqué, M., Georgievski, G., 2014. EURO-CORDEX: new high-resolution climate change projections for European impact research. Reg. Environ. Chang. 14, 563–578.
Jolly, W.M., Cochrane, M.A., Freeborn, P.H., Holden, Z.A., Brown, T.J., Williamson, G.J., Bowman, D.M., 2015. Climate-induced variations in global wildfire danger from 1979 to 2013. Nat. Commun. 6.
Kottek, M., Grieser, J., Beck, C., Rudolf, B., Rubel, F., 2006. World map of the Köppen-Geiger climate classification updated. Meteorol. Z. 15, 259–263.
Krueger, O., Hegerl, G.C., Tett, S.F., 2015. Evaluation of mechanisms of hot and cold days in climate models over Central Europe. Environ. Res. Lett. 10, 014002.
Landelius, T., Dahlgren, P., Gollvik, S., Jansson, A., Olsson, E., 2016. A high-resolution regional reanalysis for Europe. Part 2: 2D analysis of surface temperature, precipitation and wind. Q. J. R. Meteorol. Soc. 142, 2132–2142.
Lustenberger, A., Knutti, R., Fischer, E.M., 2014. The potential of pattern scaling for projecting temperature-related extreme indices. Int. J. Climatol. 34, 18–26.
Mann, H.B., Whitney, D.R., 1947. On a test of whether one of two random variables is stochastically larger than the other. Ann. Math. Stat. 50–60.
Maraun, D., Huth, R., Gutiérrez, J.M., Martín, D.S., Dubrovsky, M., Fischer, A., Hertig, E., Soares, P.M., Bartholy, J., Pongrácz, R., 2017. The VALUE perfect predictor experiment: evaluation of temporal variability. Int. J. Climatol.
Marto, N., 2005. Heat waves: health impacts. Acta Medica Port. 18, 467–474.
McGregor, G.R., Bessemoulin, P., Ebi, K.L., Menne, B., 2015. Heatwaves and Health: Guidance on Warning-System Development. World Meteorological Organization.
Miller, N.L., Hayhoe, K., Jin, J., Auffhammer, M., 2008. Climate, extreme heat, and electricity demand in California. J. Appl. Meteorol. Climatol. 47, 1834–1844.
Miralles, D.G., Teuling, A.J., Van Heerwaarden, C.C., de Arellano, J.V.-G., 2014. Megaheatwave temperatures due to combined soil desiccation and atmospheric heat accumulation. Nat. Geosci. 7, 345–349.
Monteiro, A., Velho, S., 2014. Health heat stress in the Porto metropolitan area–a matter of temperature or inadequate adaptation? ERDE–J. Geogr. Soc. Berl. 145, 80–95.
Monteiro, A., Carvalho, V., Oliveira, T., Sousa, C., 2013. Excess mortality and morbidity during the July 2006 heat wave in Porto, Portugal. Int. J. Biometeorol. 57, 155–167.
Ouzeau, G., Soubeyroux, J.-M., Schneider, M., Vautard, R., Planton, S., 2016. Heat waves analysis over France in present and future climate: application of a new method on the EURO-CORDEX ensemble. Clim. Serv. 4, 1–12.
Page, Y.L., Pereira, J.M.C., Trigo, R., da Camara, C., Oom, D., Mota, B., 2008. Global fire activity patterns (1996–2006) and climatic influence: an analysis using the world fire atlas. Atmos. Chem. Phys. 8, 1911–1924.
Parente, J., Pereira, M.G., 2016. Structural fire risk: the case of Portugal. Sci. Total Environ. 573, 883–893.
Parente, J., Pereira, M.G., Tonini, M., 2016. Space-time clustering analysis of wildfires: the influence of dataset characteristics, fire prevention policy decisions, weather and climate. Sci. Total Environ. 559, 151–165.
Pereira, M.G., 2015. Mathematics of energy and climate change: from the solar radiation to the impacts of regional projections. Mathematics of Energy and Climate Change. Springer, pp. 263–295.
Pereira, M.G., Trigo, R.M., da Camara, C.C., Pereira, J.M., Leite, S.M., 2005. Synoptic patterns associated with large summer forest fires in Portugal. Agric. For. Meteorol. 129, 11–25.
Pereira, M.G., Malamud, B.D., Trigo, R.M., Alves, P.I., 2011. The history and characteristics of the 1980-2005 Portuguese rural fire database. Nat. Hazards Earth Syst. Sci. 11, 3343.
Pereira, M.G., Calado, T.J., DaCamara, C.C., Calheiros, T., 2013. Effects of regional climate change on rural fires in Portugal. Clim. Res. 57, 187–200.
Pereira, M.G., Aranha, J., Amraoui, M., 2014. Land cover fire proneness in Europe. For. Syst. 23, 598–610.
Perkins, S.E., Alexander, L.V., 2013. On the measurement of heat waves. J. Clim. 26, 4500–4517.
Perkins, S.E., Alexander, L.V., Nairn, J.R., 2012. Increasing frequency, intensity and duration of observed global heatwaves and warm spells. Geophys. Res. Lett. 39.
Pfeifer, S., Bülow, K., Gobiet, A., Hänsler, A., Mudelsee, M., Otto, J., Rechid, D., Teichmann, C., Jacob, D., 2015. Robustness of ensemble climate projections analyzed with climate signal maps: seasonal and extreme precipitation for Germany. Atmosfera 6, 677–698.

Rebetez, M., Mayer, H., Dupont, O., Schindler, D., Gartner, K., Kropp, J.P., Menzel, A., 2006. Heat and drought 2003 in Europe: a climate synthesis. Ann. For. Sci. 63, 569–577.
Rebetez, M., Dupont, O., Giroud, M., 2009. An analysis of the July 2006 heatwave extent in Europe compared to the record year of 2003. Theor. Appl. Climatol. 95, 1–7.
Russo, S., Dosio, A., Graversen, R.G., Sillmann, J., Carrao, H., Dunbar, M.B., Singleton, A., Montagna, P., Barbola, P., Vogt, J.V., 2014. Magnitude of extreme heat waves in present climate and their projection in a warming world. J. Geophys. Res. Atmos. 119.
Russo, S., Sillmann, J., Fischer, E.M., 2015. Top ten European heatwaves since 1950 and their occurrence in the coming decades. Environ. Res. Lett. 10, 124003.
Santos, J.A., Woollings, T., Pinto, J.G., 2013. Are the winters 2010 and 2012 archetypes exhibiting extreme opposite behavior of the North Atlantic jet stream? Mon. Weather Rev. 141, 3626–3640.
Sousa, P.M., 2017. Northern Hemisphere Blockings and Their Impacts Over the European Continent-Historical Overview and Associated Mechanisms. (Doutoramento em Ciências Geofísicas e Geoinformação - Meteorologia). Universidade nova de Lisboa, Lisboa.
Sousa, P.M., Barriopedro, D., Trigo, R.M., Ramos, A.M., Nieto, R., Gimeno, L., Turkman, K.F., Liberato, M.L., 2016. Impact of Euro-Atlantic blocking patterns in Iberia precipitation using a novel high resolution dataset. Clim. Dyn. 46, 2573–2591.
Sousa, P.M., Trigo, R.M., Barriopedro, D., Soares, P.M., Santos, J.A., 2017. European temperature responses to blocking and ridge regional patterns. Clim. Dyn. 1–21.
Spinoni, J., Naumann, G., Vogt, J.V., Barbosa, P., 2015. The biggest drought events in Europe from 1950 to 2012. J. Hydrol. Reg. Stud. 3, 509–524.
Stefanon, M., D'Andrea, F., Drobinski, P., 2012. Heatwave classification over Europe and the Mediterranean region. Environ. Res. Lett. 7, 014023.
Stéfanon, M., Drobinski, P., D'Andrea, F., Lebeaupin-Brossier, C., Bastin, S., 2014. Soil moisture-temperature feedbacks at meso-scale during summer heat waves over Western Europe. Clim. Dyn. 42, 1309–1324.
Tedim, F., Leone, V., Amraoui, M., Bouillon, C., Coughlan, M., Delogu, G., Fernandes, P.M., Ferreira, C., McCaffrey, S., McGee, T., Parente, J., Paton, D., Pereira, M.G., Ribeiro, L., Viegas, D., Xanthopoulos, G., 2018. Defining extreme wildfire events: difficulties, challenges, and impacts. Firehouse 1:9. https://doi.org/10.3390/fire1010009.
Telesca, L., Pereira, M.G., 2010. Time-clustering investigation of fire temporal fluctuations in Portugal. Nat. Hazards Earth Syst. Sci. 10, 661–666.
Trigo, R.M., Pozo-Vázquez, D., Osborn, T.J., Castro-Díez, Y., Gámiz-Fortis, S., Esteban-Parra, M.J., 2004. North Atlantic oscillation influence on precipitation, river flow and water resources in the Iberian peninsula. Int. J. Climatol. 24, 925–944.
Trigo, R.M., García-Herrera, R., Díaz, J., Trigo, I.F., Valente, M.A., 2005. How exceptional was the early august 2003 heatwave in France? Geophys. Res. Lett. 32.
Trigo, R.M., Pereira, J., Pereira, M.G., Mota, B., Calado, T.J., Dacamara, C.C., Santo, F.E., 2006. Atmospheric conditions associated with the exceptional fire season of 2003 in Portugal. Int. J. Climatol. 26, 1741–1757.
van der Velde, M., Wriedt, G., Bouraoui, F., 2010. Estimating irrigation use and effects on maize yield during the 2003 heatwave in France. Agric. Ecosyst. Environ. 135, 90–97.
Van Vuuren, D.P., Edmonds, J., Kainuma, M., Riahi, K., Thomson, A., Hibbard, K., Hurtt, G.C., Kram, T., Krey, V., Lamarque, J.-F., 2011. The representative concentration pathways: an overview. Clim. Chang. 109, 5.
Vautard, R., Gobiet, A., Jacob, D., Belda, M., Colette, A., Déqué, M., Fernández, J., García-Díez, M., Goergen, K., Güttler, I., 2013. The simulation of European heat waves from an ensemble of regional climate models within the EURO-CORDEX project. Clim. Dyn. 41, 2555–2575.
WCRP CORDEX, 2016. First Bias-Adjusted CORDEX Data Now Freely Available. (WWW Document). https://www.wcrp-climate.org/news/wcrp-news/1019-first-bias-adjusted-cordex-data.
Wilcoxon, F., 1945. Individual comparisons by ranking methods. Biom. Bull. 1, 80–83.
WMO, 2016. Guidelines on the Definition and Monitoring of Extreme Weather and Climate Events: Draft Version - First Review by TT-Dewce.
Yang, W., Andréasson, J., Graham, L.P., Olsson, J., Rosberg, J., Wetterhall, F., 2010. Distribution-based scaling to improve usability of regional climate model projections for hydrological climate change impacts studies. Hydrol. Res. 41, 211–229.
You, Q., Kang, S., Pepin, N., Flügel, W.-A., Yan, Y., Behrawan, H., Huang, J., 2010. Relationship between temperature trend magnitude, elevation and mean temperature in the Tibetan plateau from homogenized surface stations and reanalysis data. Glob. Planet. Chang. 71, 124–133.